script)
= deviation from the steady state value (as superscript)

LITERATURE CITED

1. Bollinger, R. E., and D. E. Lamb, *Chem. Eng. Progr. Symp. Ser. No. 55*, **61**, 66 (1965).
2. Chen, K., R. A. Mathias, and M. D. Sauter, *Trans. AIEE* **82**, 336 (1962).
3. Distefano, G. P., *AIChE J.*, **14**, 190 (1968).
4. Falb, P. L., and W. A. Wolovich, *Trans. IEEE Automatic Control*, **AC-12** (6), 651 (1967).
5. Foster, R. D., and W. F. Stevens, *AIChE J.*, 13, (2), 334 (1967).
6. Freeman, H., *Trans. AIEE*, **77**, 1 (1958).
7. Gilbert, E. G., "The Decoupling of Multivariable Systems by State Feedback," Univ. Michigan, Ann Arbor (1968).
8. Greenfield, G. G., and T. J. Ward, *Ind. Eng. Chem. Fundamentals*, **6**, (4), 564 (1967).
9. *Ibid.*, **6**, 571 (1967).
10. Kavanagh, R. J., *J. Franklin Inst.*, **262**, 349 (1956).
11. Kleinpeter, J. A., Ph.D. dissertation, Tulane Univ., New Orleans, La. (1968).
12. Liu, S., *Ind. Eng. Chem. Process Design Develop.*, **6**, 460 (1967).
13. Luyben, W. L., and D. E. Lamb, *Chem. Eng. Progr., Symp. Ser. No. 46*, **59** (1963).
14. Morgan, B. S., *Trans. IEEE*, **AC-9**, 405 (1964).
15. Planchard, J. A., Jr., Ph..D dissertation, Tulane Univ., New Orleans, La. (1967).
16. Rich, S. E., Ph.D. dissertation, Tulane Univ., New Orleans, La. (1970).
17. Tinkler, J. D., Ph.D. dissertation, Univ. Delaware, Newark (1967).

Manuscript received February 14, 1969; revision received April 1, 1970; paper accepted April 6, 1970. Paper presented at AIChE New Orleans meeting.

Velocity and Turbulence Measurements of Air Flow Through A Packed Bed

D. F. VAN DER MERWE and W. H. GAUVIN

Mean velocity and turbulence measurements in the void spaces of a cubic packing of equal spheres have been made at Reynolds numbers of 27,000, 10,000, 5,000 and 2,500, where N_{Re} is based on superficial air velocity and a sphere diameter of 7 cm. Two cubic arrangements were used: in the regular arrangement, the mean flow was parallel to one of the principal axes, while in the skewed arrangement, the mean flow made equal angles with the three principal axes of the packing.

Transverse mean velocity and turbulence intensity profiles across the center line of a central pore have been measured behind every bank and behind the bed for the regular arrangement of ten banks of spheres. The power spectrum and probability distribution of the fluctuating velocity have also been determined.

In a previous study (*1*) measurements of the pressure distribution on a sphere in a packed bed of uniform spheres in the cubic arrangement have shown that, generally speaking, the boundary-layer behavior on a sphere in a packing remains similar to that over a single sphere, when allowance is made for the effects of turbulence and of pressure gradient. The following qualitative description of the flow was deduced from the results: The laminar boundary layer on a sphere in the first bank separates at an angle ψ (measured from the front stagnation point) of about 90

D. F. van der Merwe is at the University of the Witwatersrand, Johannesburg, South Africa. W. H. Gauvin is with Noranda Research Centre, Pointe Claire, Quebec, Canada.

deg. It reattaches on the second sphere at ψ of about 30 deg. The spreading of the jet in the first pore is relatively small, the potential core forming a large part of the jet cross section. In the second pore the potential core is smaller, the turbulence level is higher, and the jet boundary is more diffuse. The boundary layer on the second and subsequent spheres in the bed is turbulent and separates at ψ of about 130 deg. on the second sphere, and somewhat later in the body of the packed bed, with reattachment at ψ of about 40 deg. This trend continues in subsequent banks but with diminishing effect, the pressure distribution for the fifth and sixth layers appearing to be quite similar. Over the final (tenth bank of spheres in this experiment) the sudden change in the pressure gradient due to the abrupt expansion of the flow is expected to diminish the measured pressure drag coefficient. This picture is qualitatively in accord with the known experimental results on the effect of turbulence on the drag coefficient of single spheres (2, 3).

The study also showed that a considerably longer cubic packing is required that has been deemed necessary by a number of other investigations to obtain an environment for a sphere that is representative of a large bed, due to the very large pressure drag of the first upstream bank of spheres.

Finally, it was shown that when the orientation of the cubic packing was changed, so that the mean air flow direction made equal angles with the three principal axes of the packing (the skewed arrangement), the overall pressure drop of the bed was less than for the regular arrangement—which is certainly contrary to expectation—and the sphere pressure drag coefficients were also less.

The present paper is concerned with the detailed study of the mean velocity distribution and of the turbulence characteristics in the pores of the packing. This knowledge is essential for accurate predictions of heat or mass transfer from the particles forming the packing, as well as to calculate mixing or reaction rates in a packed bed. Previous work of this nature is not plentiful. Prausnitz and Wilhelm (4) have given the first account of the measurements of mean and fluctuating velocities in a packed bed. They found that the measurements behind the bed bore little resemblance to the measurements inside it. They used a rhombohedral packing of 1.5-in. diam. spheres, 11 layers deep in a 12-in. sq. duct. Measurements at Reynolds numbers of 4,870 and 7,010 were made behind the seventh layer. The turbulence intensity was found to be as high as 50%, and the one-dimensional spectra appeared to be similar to the one-dimensional spectra measured in isotropic turbulence. Nevertheless, the dispersion produced by the turbulence according to Taylor's theory (6) was much less than the dispersion found from the displacement of a tracer. They attributed the relatively lower heat transfer rates found near contact points to lower velocities and turbulence intensities. The otherwise increased overall heat transfer rates were not ascribed to regular eddy shedding, which had not been found to occur.

Jolls (7) studied the local mass transfer coefficient on the surface of a 1-in. diam. sphere in a dumped packing filling a cylinder 12 in. wide and 60 in. long. The transition to turbulence was established to occur at $N_{Re} = 115$. Correlation measurements of the local mass transfer fluctuations between two points on the surface of the sphere showed the existence of large-scale velocity fluctuations outside wake-flow regions on the sphere.

EXPERIMENT

The experimental equipment is shown diagrammatically in Figure 1, and is described in greater detail in reference 1. The packed bed consisted of two cubic packings of equal spheres: in the first, termed the regular arrangement, the mean flow direction was parallel to one of the principal axes of the packing, while in the other, called the skewed arrangement, the mean flow made equal angles with the three principal axes of the packing. The regular arrangement consisted of ten banks of 70-mm. diam. spheres, spun from aluminum, a single bank being formed by nine full spheres with half and quarter spheres to fill in the side of the 28-cm. sq. Lucite frame. In the skewed arrangement the length of the bed was about 14 sphere diameters.

It is convenient to describe the geometry of the regular bed with reference to the two coordinate systems shown in Figure 2. X, Y, Z gives the position of the center of the spheres measured in sphere diameters in from the central sphere in the first bank, and x,y,z is a local coordinate system describing the location in the void (also measured in sphere diameters), the origin being centrally located between the four spheres forming the void behind the central sphere. Thus coordinates X,Y,Z of 5.5, 0.5, 0.5 and x,y,z of 0,0,0.14 denote the point in the central pore behind the sixth sphere (in the direction of mean flow) located 0.14 diam. in a horizontal direction from the center of the pore, transverse to the mean flow.

The purpose of the experimental study was to measure the mean velocity and turbulence intensity at four points spaced across the center line that traverses laterally one-half the void space adjoining the central sphere of a bank. These measurements were to be made in the corresponding void space behind every bank in the bed, and also behind the bed. Further analysis of the turbulence to yield the power spectrum and the probability density of the fluctuating velocity was to be made. Also to be attempted was an estimate of the longitudinal macroscale of the turbulence. In addition, the same measurements were to be made in the skewed arrangement, but were limited to the traverse of a single void in the center of the bed. The program of measurements was to be repeated at four nominal Reynolds numbers: 27,000, 10,000, 5,000 and 2,500.

These measurements will not give the detailed local description of the shear flow outside and in the boundary layer required for the exact calculation of transfer coefficients. Instead,

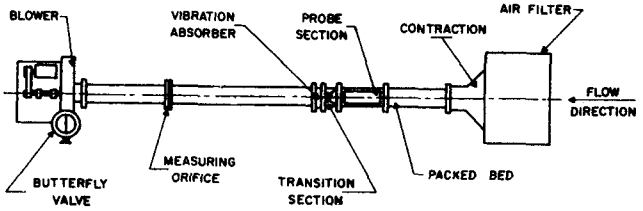

Fig. 1. Diagram of experimental equipment.

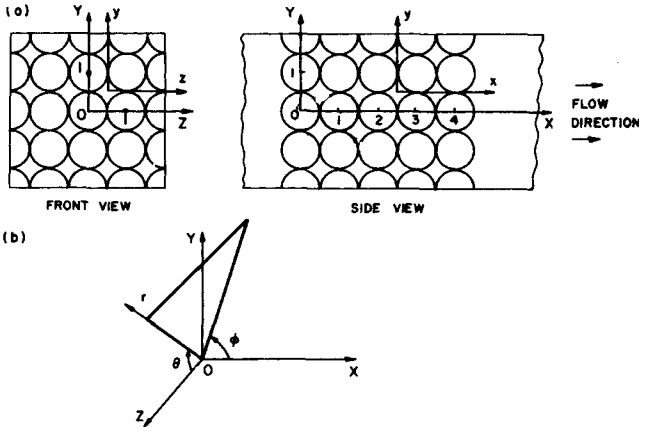

Fig. 2. Coordinate systems used in packed bed. (a) Rectangular coordinate systems: (X,Y,Z) specify location in bed; (x,y,z) specify location in pore. (b) Spherical coordinate system.

it is aimed at providing a larger, if more superficial, description of the flow inside a packing, the characteristics of which are little known.

Instrumentation

A DISA constant-temperature anemometer Type 55A01, with DISA miniature velocity probes Type 55A25, provided the voltage signals from which the mean and fluctuating velocities were obtained.

The bridge voltage of the DISA anemometer was fed into an L-3 linearizer supplied by L. T. Miller, Baltimore, Md. The fluctuating parts of the anemometer bridge output, as well as the linearizer output, were measured on a DISA random signal indicator and correlator, Type 55A06. The mean values of the bridge voltage and the linearizer output were measured on an integrating device consisting of a timer (set for 100 sec.) and a Hewlett-Packard voltage-to-frequency converter No. 2210, and a Hewlett-Packard five-digit counter No. 3734A. These measurements formed the basis for calculating the turbulence intensities. The DISA random signal correlator also included a time-differentiation device, and by measuring the ratio of the root-mean-square of the input signal and the root-mean-square of the time-differentiated input signal, a measure of the microscale (Taylor dissipation length scale) was obtained. The latter measurements are not reported here, however, since they are semiquantitative in nature, as the length of the wire used was larger than the Kolmogoroff microscale η. To provide an adequate resolution of the velocity field in the inertial subrange, the wire length should be shorter than η (*12*).

The fluctuating output of the linearizer, as well as the time-differentiated fluctuating linearizer output, were FM-recorded on an AMPEX SP-300 magnetic tape recorder/reproducer at 15 inputs/sec. These signals were later transferred to 38-ft. long closed loops on an AMPEX FL-200 closed-loop recorder/reproducer at 15 inputs/sec. The closed loops were played back at 60 inputs/sec. to obtain the power spectral density on a Honeywell 9050 automatic wave analyzer, and, simultaneously, the probability density of the amplitude on a Bruel and Kjaer probability density analyzer Model 160 with an *XY* plotter.

Procedure

The flow through the packed bed was adjusted to the appropriate Reynolds number as described in reference *1*. At the same time a hot-wire probe was calibrated in a jet issuing from a 0.25-in. diam. orifice. The orifice had a rounded entrance and was located at the end of a 9-ft. long, 1-in. diam. horizontal glass tube. Three sizes of rotameter, previously calibrated against a wet-test meter when supplied from compressed gas cylinders, allowed the adjustment of the velocity from 20 to 2,000 cm./sec. The temperature of the gas was measured ahead of the orifice.

The velocity probe could be rotated to calibrate the probe's angular response, and two further sizes of orifice were available to extend the velocity measurements to lower values, direct measurement of the velocity in the center of the tube being possible for very low velocities.

The hot-wire filaments were washed in methanol and carbon tetrachloride, allowed to dry, and were then placed in the jet for calibration. All the hot wires were operated at a resistance ratio of 1:8 during calibration, as well as during measurements in the bed. The calibration consisted of a record of the velocity versus the mean voltage of the linearizer, as well as the mean bridge voltage of the anemometer, together with the gas temperature and the cold resistance of the wire. In effect, one obtained in this way a calibration for the hot-wire filament as well as a calibration for the linearizer, which was extremely sensitive to changes in temperature. Immediately following the calibration the probe was used for measurements in the bed. Experience showed that the wire calibration remained unaffected by use in the bed, but the linearizer required calibration before every run.

The accurate location of the probe in the pore was established by initially locating the probe at the center of the pore. The vernier-controlled, sliding supports on the side were first adjusted to introduce the probe at the correct level (the xz plane in pore coordinates), and then by sighting between two crosses marked on the top and bottom of the Lucite frame at the center of the pore, to fix the location in the xz plane.

Reduction of Hot-Wire Measurements

It can be shown (*8*) that all components of the Reynolds stress tensor can be determined without approximation, within the experimental accuracy, through suitable electronic manipulation of the hot-wire anemometer output signal. In general, the outputs of the anemometer $V^* = \overline{V}^* + v^*$ and of the linearizer $E = \overline{E} + e$ require corrections for the contributions of the mean square fluctuating signal to the measured mean values $\overline{V}^*$ and $\overline{E}$ to determine the mean voltages $\overline{V}^*_c$, $\overline{E}_c$ that will correspond to the magnitude $\overline{Q}_c$ of the effective mean velocity as has been found in the calibration of the wire. Rose (*9*), Champagne (*10*), and Heskestad (*11*) have given appropriate procedures.

In the following, the mean value of a quantity will be denoted by an overbar and its root-mean-square value by a prime. In this exploratory survey of flow properties in a packed bed the aim was to determine the local velocity $\overline{U}$ in the X, x direction. Since all measurements were made along a centerline of the void or pore, in a horizontal direction transverse to the flow, $\overline{u}^2 = \overline{v}^2 = \overline{w}^2$ was assumed in order to make an estimate of the first-order correction. The hot wire was always operated at the same ratio (1.8:1) of operating to cold resistance of the wire, and corrections have been made for temperature differences between calibration and operating conditions. In addition, it has been assumed that the wire responds only to the component of the velocity normal to it. Denote the local longitudinal turbulence intensity by $I = u'/\overline{U}$. Turbulence is absent under calibration conditions, and the equation for the linearizer output

$$\overline{E} = K^* Q^M \tag{1}$$

becomes

$$\overline{E}_c = K^* \overline{Q}_c^M$$

where $\overline{Q}_c$ denotes the magnitude of the mean velocity that corresponds to $\overline{E}_c$ under calibration conditions. The exponent $M = 1$ if the linearizer operates satisfactorily, and deviation of M of more than 2% from unity, would render the calibration unacceptable. The linearizer output E is written as

$$\overline{E} = \overline{E}_c + (\partial \overline{E}/\partial R)_c \, \delta R + (\partial \overline{E}/\partial Q)_c \, \delta Q \ . \ . \ . \tag{2}$$

where R is the operating resistance of the hot wire. $\delta R = R - R_c$ = change in operating resistance due to temperature change. $\delta Q = \overline{Q} - \overline{Q}_c$ = contribution of turbulence to measured value of velocity. The nonlinear voltage V^* across the wire may be written as

$$V^* = R(A + BQ^N) = RBQ^N P \tag{3}$$

where

$$P = 1 + (A/BQ^N) \tag{4}$$

Write $\Delta Q = \delta Q/\overline{Q}_c$; then

$$(\Delta Q)' = I = u'/\overline{U} \tag{5}$$

and

$$\overline{\Delta Q} = 0.5 \ I^2, \text{ to the first order} \tag{6}$$

Higher orders of approximation require more electronic gadgetry to multiply signals, or use a gaussian hypothesis to relate higher order moments of the velocity to lower orders and to neglect others.

Approximate I by $I_0 = e'/\overline{E}$. The correct value of the turbulence intensity is $I = e'/\overline{E}_c$, where $\overline{E}_c$ is given by (to the first order)

$$E_c = \overline{E}(1 - 0.5 \ I_0 I)/(1 + (M/N)P\Delta R) \tag{7}$$

where

$$\Delta R = (R - R_c)/R_c$$

An iteration procedure is used to find I, P and $\overline{E}_c$.†

Accuracy of Measurements

It is unfortunately true that the measured values of the turbulence intensity are affected by the choice of the hot-wire response that is assumed and the corrections that are applied after allowing for instrumentation limitations. A second limitation is imposed by the absolute accuracy of the velocity determined in the calibration rig, which may be of the order of 5%. Nevertheless, mean velocity measurements relative to the velocity standard of the calibration can be made with a precision of about 0.2%. Turbulence measurements can be made on the anemometer with a precision of 2% and ratio measurements with a precision of 5%. Another factor whose influence remains undetermined is the irregular change in the mean flow pattern, which will be described in the following section. For the particular type of turbulence that is assumed to be measured, the intensity and mean velocities (relative to the velocity of the calibration rig) are measured with a precision of 2% under favorable conditions, that is, no rapid change occurring in the mean flow pattern. The accuracy under favorable circumstances is of the order of 5%, and closer to 15% if the special assumptions listed above are considered.

The spectral analysis of the fluctuating signal has been made with the equivalent number of degrees of freedom being 224, or a normalized mean square error of 0.095. The analysis of the probability density has an accuracy of the same order. The comparatively high resolution of the fluctuating signal obtained in the spectral analysis does not imply that the longitudinal spectral density function $f(k)$ is known with the same accuracy.

There are at least two additional sources of error to consider. The first involves the resolution of the fluctuating velocity field by the hot-wire filament. It was found that the hot-wire filament does not fulfill the "short-wire" (*12*) approximation, but the "long-wire" approximation was well satisfied. The required corrections for the long-wire approximation have been given by Uberoi and Kovasznay (*13*), but have not been applied. However, wave numbers up to 4.3 and 2.9 cm.$^{-1}$ can be resolved by the filament at $N_{Re} = 27{,}000$ and $N_{Re} = 2{,}500$, respectively. This corresponds to frequencies of 1,300 and 150 hz., respectively, which are well within the 2,000-hz. bandwidth of the recorder/reproducer.

The second source of error involves the correctness of the transformation of frequency n (in herzs) to wave number k.

$$k = 2\pi n/\overline{U} \tag{8}$$

This equation implies that the turbulence is convected in a "frozen" pattern past the observation point, and is known as Taylor's hypothesis (*6*). Lin (*14*), Corrsin (*15*), and Lumley (*16*) have discussed the applicability of the hypothesis to shear flows. Heskestad (*11*) proposed a modification of Taylor's hypothesis for high Reynolds number turbulent shear flow. Since neither the turbulent shear stresses nor the turbulent normal stresses have been determined, the application is precluded of both Lumley's criteria for isotropy and the neglect of fluctuations of the convection velocity, and Heskestad's correction factor. Regardless of whether one interprets the spectrum in terms of frequency, rather than wave number, and the velocity as a function of time, rather than position, one uses the same combination of variables in forming dimensionless parameters such as the Reynolds number of the turbulence. This motivates, and justifies, the use of transformation (8), without sanctioning an interpretation other than a formalistic procedure.

Flow Visualization

Flow visualization at the lowest Reynolds number with a mixture of talc powder and paraffin oil indicated a separation of the flow at $\Psi = 90$ deg. on the first sphere and left spiral traces seemingly indicating large vortices in the four quadrants of the downstream portion of the sphere in the regular arrangement. Attaching tufts of down to a smooth, black-painted sphere confirmed this picture but also indicated that the flow was subject to sudden changes at irregular intervals; the strength or size of the vortices in two quadrants would alternate between greater or smaller values. At higher Reynolds numbers, this fluctuating but regular pattern disappeared as the fluctuations increased in frequency. At the highest Reynolds number no regular pattern could be observed but rapid alteration of the direction of tufts located at Ψ just larger than 90 deg. was observed, indicating a changing pattern in the separating and attaching flows.

The observed flow behavior seems to indicate that one should think in terms of an average mean flow and turbulence pattern in the packed bed.

Experimental Results

Experimental values of $\overline{U}$ (the mean local velocity in the x direction), I (the intensity of turbulence $u'/\overline{U}$), K (the flatness factor of the probability density function of the fluctuating velocity u), and K' (the flatness factor of the probability density function of the time derivative of u) are given for the regular arrangement in Tables 1*A* through 1*D*, for Reynolds numbers of 2,500, 5,000, 10,000 and 27,000 respectively.* Measurements were made in the central pore following each bank of spheres, and also 1.5 sphere diameter behind the bed of ten banks. Values for the skewed arrangement at the same Reynolds numbers are shown in Tables 2*A* to 2*D*. They were made in a single pore located in the center of the bed. However, the value denoted by $\overline{U}$ now has the significance of being the magnitude of the normal component of the mean velocity to the hot-wire filament, and the root-mean-square value u' is the magnitude of the fluctuating velocity in the direction of the mean velocity normal to the wire.

A few typical spectra of the fluctuating velocity are shown in Figure 3. In these, the spectral density $F(k)$ is arbitrarily scaled, and the wave number k has been obtained through the formal transformation given in Equation (8).

Transverse normalized mean velocity profiles are shown in Figures 4 and 5 for Reynolds numbers of 2,500 and 27,000 respectively. Figure 6 shows the variation of turbulence intensity measured at pore centers in a longitudinal direction along the bed. Finally, Figure 7 shows the transverse turbulence intensity profiles across the pore centers in each bank, at $N_{Re} = 27{,}000$.

DISCUSSION OF RESULTS

Mean Flow in the Packed Bed

The measurements of the mean velocity are shown in Figure 4 for $N_{Re} = 2{,}500$ and in Figure 5 for $N_{Re} = 27{,}000$. Apart from the vastly different velocity profiles behind the bed, the shape of the velocity profile changes from pore to pore, for $N_{Re} = 2{,}500$. Inspection of the measurements at $N_{Re} = 5{,}000$ and $N_{Re} = 10{,}000$ in Tables 1*B* and 1*C* shows that the velocity maximum occasionally occurs away from the center of the pore, indicating slightly asymmetrical flow. Apart from the observed changes in mean velocity pattern already commented upon, this behavior could also be the result of slight differences in alignment between the various banks that make up the packed bed.

The flow at $Y = 0.5$, $Z = 0.5$, $X = 0.5$, 1.5, etc., is reversed when $z = 0.5$, and a standing eddy is expected.

† For a complete derivation of Equation (7), see reference *8*.

* Tables 1A through 1D have been deposited as document 01383 with the ASIS National Auxiliary Publications Service, c/o CCM Information Sciences, Inc., 909 Third Ave., New York 10022 and may be obtained for $2.00 for microfiche or $5.00 for photocopies.

The pressure distributions reported in reference *1* also bear out this interpretation, the stagnation point for the flow being located at a value of ψ of approximately 25 deg. The mean velocity profiles appear to be more peaked at N_{Re} = 27,000 than at N_{Re} = 2,500. This is contrary to the trend observed in pipe flow where the velocity profile tends to become flatter at higher Reynolds numbers. One notes that the relative magnitude of the back flow is also higher at N_{Re} = 27,000 as compared to N_{Re} = 2,500.

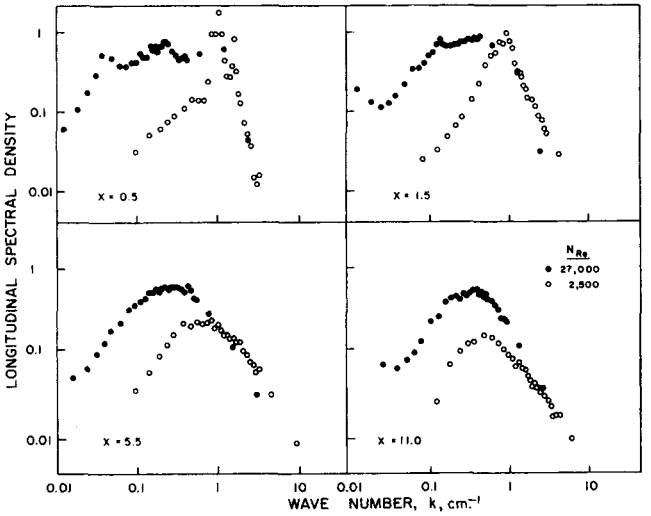

Fig. 3. Spectra measured in packed bed at the highest and lowest Reynolds number.

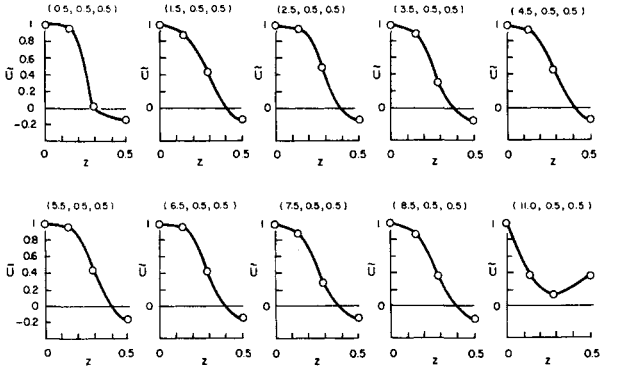

Fig. 4. Transverse normalized mean velocity profiles across the pore centers (N_{Re} = 2,500).

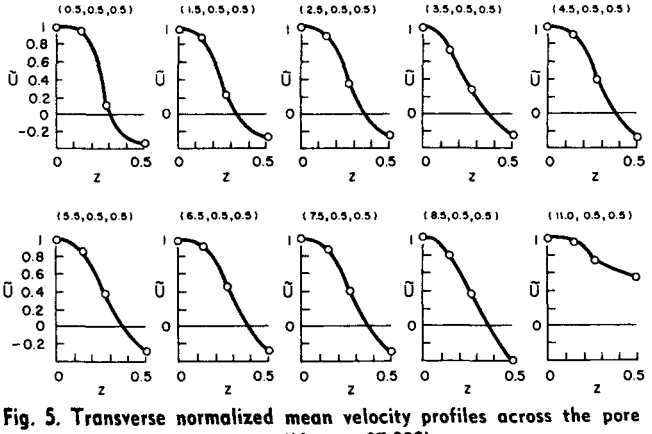

Fig. 5. Transverse normalized mean velocity profiles across the pore centers (N_{Re} = 27,000).

Comparison with velocities measured in the skewed arrangement is difficult, since the superficial velocity now makes equal angles with the principal axes of the packing which are parallel to the x, y, z axes in the pore, and it is clear that the flow through a void is not symmetric. This rules out the analysis that is possible for the regular arrangement. However, since all six openings to a pore in the skewed arrangement are now available for flow, the

TABLE 2. SKEWED ARRANGEMENT

Center coordinates X	Y	Z	Pore coordinates x	y	z	$\overline{U}$, cm./sec.	I	K	K'
A. Mean velocities and turbulence parameters N_{Re} = 2,500									
Central pore of skewed arrangement	0	0	−0.43			144	0.331		
	0	0	−0.28			97	0.393		
ϕ = 90 deg.	0	0	−0.14			73	0.500		
θ = 90 deg.	0	0	0			102	0.437	3.39	3.96
Hot-wire orientation	0	0	0.14			127	0.391	2.99	3.68
	0	0	0.28			190	0.279	3.02	3.457
	0	0	0.43			264	0.212	3.08	3.74
	0	0	0.57			74	0.573		
B. Mean velocities and turbulence parameters N_{Re} = 5,000									
Central pore of skewed arrangement	0	0	−0.43			282	0.391		
	0	0	−0.28			169	0.476		
ϕ = 90 deg.	0	0	−0.14			144	0.546		
θ = 90 deg.	0	0	0			187	0.522	2.92	3.45
Hot-wire orientation	0	0	0.14			229	0.480	2.84	3.42
	0	0	0.28			363	0.328	2.80	2.86
	0	0	0.43			529	0.211	2.85	3.56
	0	0	0.57			133	0.684		
Central pore of skewed arrangement	0	0	−0.43			318	0.312		
	0	0	−0.28			246	0.370		
ϕ = 135 deg.	0	0	−0.14			201	0.416		
θ = 90 deg.	0	0	0			181	0.506		
Hot-wire orientation	0	0	0.14			183	0.483		
	0	0	0.28			276	0.313		
	0	0	0.43			410	0.216		
	0	0	0.57			130	0.680		
C. Mean velocities and turbulence parameters N_{Re} = 10,000									
Central pore of skewed arrangement	0	0	−0.43			554	0.305		
	0	0	−0.28			384	0.361		
ϕ = 90 deg.	0	0	−0.14			326	0.420		
θ = 90 deg.	0	0	0			379	0.426	2.91	3.40
Hot-wire orientation	0	0	0.14			439	0.400	2.85	3.44
	0	0	0.28			606	0.282	2.78	2.90
	0	0	0.43			826	0.205	2.92	3.18
	0	0	0.57			430	0.434		
D. Mean velocities and turbulence parameters N_{Re} = 27,000									
Central pore of skewed arrangement	0	0	−0.43			1,322	0.321		
	0	0	−0.28			876	0.407		
ϕ = 90 deg.	0	0	−0.14			731	0.444		
θ = 90 deg.	0	0	0			852	0.445	2.62	3.21
Hot-wire orientation	0	0	0.14			1,019	0.417	2.58	3.11
	0	0	0.28			1,322	0.321	2.83	3.06
	0	0	0.43			1,792	0.237	2.70	3.14
	0	0	0.57			1,318	0.363		

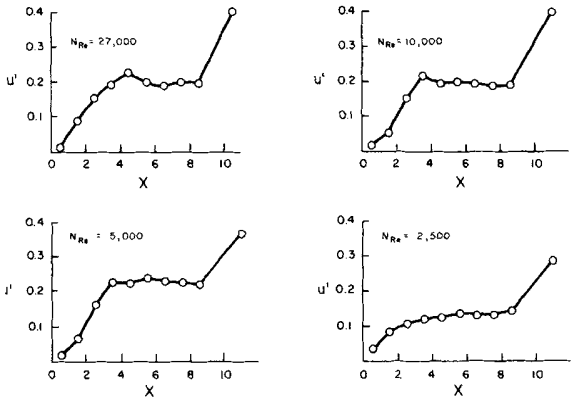

Fig. 6. Variation of turbulence intensity at pore centers along the bed for four Reynolds numbers.

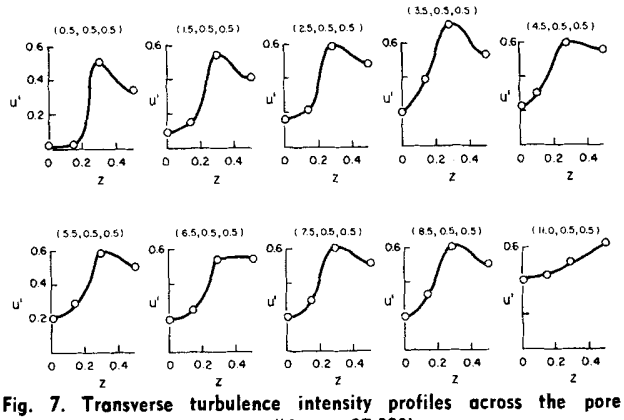

Fig. 7. Transverse turbulence intensity profiles across the pore centers (N_{Re} = 27,000).

velocity profile is clearly flatter than in the regular arrangement, and there is no apparent evidence of standing eddies.

Turbulence Intensity in Packed Bed

The variation of turbulence intensity along the length of the bed is shown in Figure 6 for the four Reynolds numbers. The values shown are those in the center of the central pore behind every bank and also 1.5 sphere diameter behind the bed. Figure 7 shows the transverse intensity profiles at N_{Re} = 27,000. The higher turbulence intensities in the pore center for N_{Re} = 5,000 shown in Figure 6 should not be taken at face value, as it may be due to an asymmetry in the flow. However, the turbulence intensity at N_{Re} = 2,500 is definitely lower than at all other Reynolds numbers. Mickley, Smith, and Korchak (5) in measurements in a rhombohedral packing found the local turbulence intensities at N_{Re} = 4,780 to be generally higher than at N_{Re} = 7,010, being 55 and 40%, respectively, in the central region of the void. The flow configurations are very different, and the relative minimum in the velocity profile for the void center found by these authors corresponds to the region away from the void center in the present measurements, where intensities of a similar magnitude are measured. They obtained intensities of 26 and 24% for Reynolds numbers of 4,780 and 7,010, respectively, away from the void center and close to the point of maximum velocity. These values are in qualitative agreement with those obtained in the present study.

The very high turbulence intensities attained at a value of z of about 0.3 should be noted in Figure 7. These high values confirm the laminar-turbulent transition in the boundary layer which was inferred from the measurements of pressure distribution in reference 1.

Spectrum of Longitudinal Velocity Fluctuations

Typical spectra inside and outside the bed are shown in Figure 3. They illustrate the behavior at two Reynolds numbers (2,500 and 27,000) in the central pores following the first, second, and sixth spheres in the bed and also behind the bed, as indicated by the value of X. Their most outstanding general characteristic is the pronounced maximum which they exhibit. This is in contrast with the usual shape of the spectrum of longitudinal fluctuations in isotropic turbulence, which remains approximately constant at low wave numbers and falls off at higher Reynolds number with increasing steepness.

The theoretical expressions for the spectrum of turbulence apply to a three-dimensional spectrum. The longitudinal one-dimensional spectrum may be used to calculate the corresponding three-dimensional spectrum when isotropy is assumed. One finds that for any particular exponent m, a relation for the three-dimensional spectrum $E(k) \sim k^m$ will imply that the one-dimensional longitudinal spectrum obeys $F(k) \sim k^m$. In principle one possesses a method to investigate the three-dimensional spectrum through the one-dimensional, experimentally determined spectrum. However, since the large-scale structure of the turbulence is not expected to be isotropic (it is formed in a regular rather than a random manner), this transformation is useful only for the universal equilibrium range of the spectrum, the small-scale structure being isotropic by assumption. In addition, the calculation involves the second derivatives of the measured spectrum, and leads to greatly amplified errors in the calculated results.

To overcome this difficulty, a smooth rational function has been fitted to the experimental points of the spectrum, using a library program of the SDS-920 computer (17). Unfortunately, the manner in which the points of the spectrum are weighted in the fitting procedure leads to uncertainties in the low and high wave number regions of the spectrum, and makes the Fourier inversion of the spectrum not profitable. Fitting the rational function approximations to the spectra has shown that, except for N_{Re} = 5,000, the same form of function

$$F(k) = (a_0 + a_1k^2)/(1 + b_1k^2 + b_2k^4 + b_3k^6 + b_4k^8) \quad (9)$$

will fit all the spectra. For N_{Re} = 5,000, the experimental points consistently show a lower decrease with wave number after the maximum in the spectrum, and before eventually tending to the same slope as the other spectra. It is not clear whether this behavior of the longitudinal spectral density function is in any way connected with the seemingly higher intensities of turbulence observed at N_{Re} = 5,000.

Eddy Shedding in Packed Bed

The resolution of the spectrum is such that eddy shedding can be observed, if it exists, this shedding presumably giving rise to a peak in the spectral density curve. For Reynolds numbers of 2,500, 5,000 and 10,000, two or more distinct peaks are observed in the void behind the first bank, for example, at N_{Re} = 2,500, see Figure 3, X = 0.5; but in the pore behind the second bank (X = 1.5) all but one of the peaks have disappeared. At the lowest Reynolds number, 2,500, there is virtually no contribution to the energy at low frequencies. There is a broad peak at 53 hz., with two small peaks on either side, followed by a second peak at 85 hz. The spectrum then falls rapidly

to the noise level at ca. 160 hz. Behind the second bank, only the first peak at 53 hz. remains, and the spectrum contains more energy at both higher and lower frequencies than does the spectrum behind the first bank. For $N_{Re} = 10{,}000$, peaks occur at 132 and 170 hz. At the highest $N_{Re} = 27{,}000$, the spectrum rises very quickly to a plateau beginning at about 10 hz. and ending at 450 hz., and then decreases steeply to the noise level at ca. 1,000 hz. Thus eddy shedding occurs at the lowest Reynolds numbers, and behind the first bank only.

Mickley, Smith, and Korchak (5) have not found eddy shedding to occur inside the packing, and their measured spectra have the appearance of the one-dimensional longitudinal spectra in isotropic turbulence. Their spectra one sphere-diameter downstream of the packing do not resemble the spectra inside the packing, and show small humps. The spectra that have been measured here at a distance of 1.5 sphere-diameter downstream of the packing do not show any peaks (see Figure 3, $X = 11$). At the lower Reynolds numbers, a rapid rise to the maximum value is observed to occur, the maximum being attained at a generally lower frequency than the corresponding maximum on a spectral density curve obtained inside the packing at the same Reynolds number. The spectrum at a Reynolds number of 27,000 shows a well-rounded hump.

One may calculate Strouhal numbers based on the peaks observed in the spectra. For $N_{Re} = 2{,}500$, if the characteristic velocity in the Strouhal number is taken on the average pore velocity $v_0 = U_0/P_0$ (where $P_0 = 0.476$ for a cubic packing), the values of the Strouhal number, nd/v_0, for the first (53 hz.) and second (85 hz.) peaks are 3.14 and 5.03, respectively. Compared to the Strouhal numbers of single spheres at the same Reynolds number proposed by Cometta (18), these values are far too high. Since the velocity profile in the center of the pore behind the first bank is quite flat, it is more logical to use the mean velocity in the center of the pore, $\overline{U} = 331$ cm./sec. (see Table 1A) to compute the Strouhal number $nd/\overline{U}$, and the respective values of 1.12 and 1.80 are obtained. These values are plausible if one can ascribe greater stability to the flow around the sphere in the first bank than to the flow around a single sphere. This is indeed the case on account of the favorable pressure gradient over the upstream part of the sphere which inhibits separation at angles $\psi < 90$ deg., where ψ is the angle from the front stagnation point.

General Appearance of the Longitudinal Spectrum

The peaked appearance of the spectra shown in Figure 3 is considered to be plausible. From Figure 6 it is seen that the turbulence intensity levels off after a number of banks. One does not expect the turbulence intensity to increase indefinitely, but rather that a balance between turbulent energy production and dissipation would be established. It follows that the energy loss through dissipation is periodically replenished with a spatial scale equal to one sphere diameter and a frequency proportional to d/v_0. With the formal transformation to wave number, using the local mean velocity, one would expect to find the peaks in the spectrum to occur at roughly the same wave number. This would be strictly true if the velocity profiles were similar at all Reynolds numbers, but the velocity profiles appear to be more peaked at the highest Reynolds number, as compared to the lowest Reynolds number, and will give a relatively lower value of the wave number for the peak at the highest Reynolds number. In addition, the spectra at lower Reynolds numbers appear to be narrower than at the highest Reynolds number of 27,000. In fact, from comparing spectra at different locations in the pore for the same Reynolds number, it appears that the turbulence spectra become narrower with decreasing turbulence Reynolds number.

To make a more specific analysis, let the frequency for the maximum in the longitudinal spectrum be n_e. The pertinent parameters that affect n_e are selected to be Δp, U_0, u_c', d, ρ, and μ. Dimensional analysis is not particularly helpful, since only the obvious dimensionless numbers such as Reynolds number, Strouhal number, turbulence intensity, and pressure loss coefficient are obtained. More specific assumptions regarding the turbulent flow are required along the lines of Owen's analysis (19) of the buffeting of boiler tubes. Owen makes it clear that his analysis for the dominant frequency of turbulent flow through tube bundles will not apply to flow through a cubic packing. Nevertheless, it is believed that the pertinent variables remain the same, and may form a useful basis for an investigation of turbulent flow through a packed bed.

Assume that the Reynolds number is sufficiently large so that the large eddies are independent of the fluid viscosity, being well separated from the small eddies that are responsible for viscous dissipation. The energy dissipation is determined by the rate at which energy is lost by the large eddies, which is determined by the structure of the energy-carrying eddies. If L_e is the length scale of the energy-carrying eddies, and u' the root-mean-square value of the turbulence velocity, then, from dimensional considerations, the energy dissipation per unit volume ϵ, is given by

$$\epsilon = Cu'^3/L_e \tag{10}$$

The constant C depends on the particular flow, but is usually of the order of unity.

The rate of energy loss in flow through the void is $\Delta u d^2 U_0$, and can be expressed in terms of a drag coefficient C_D, giving: $0.5\sigma C_D d^2 \rho U_0^3$, where σ is the solidity of the bank of spheres. Equating the rate of energy loss in flow through the void to the energy dissipation in the void yields

$$C'u'^3 d^3/L_e = 0.5\sigma C_D d^2 \rho U_0^3 \tag{11}$$

where C' will relate u' and L_e to average values in the void. The superficial velocity is not a realistic velocity to characterize the flow in the void, and one may introduce a characteristic velocity v_c through the relation

$$U_0 = \beta v_c \tag{12}$$

where β will depend on the Reynolds number in general.

The characteristic frequency n_e for eddies of size L_e is

$$n_e = v_c/L_e \tag{13}$$

and one obtains

$$dn_e/v_c = C_D(\sigma\beta^3/2C')(v_c/u')^3 \tag{14}$$

that is

$$\text{Strouhal number} \sim (\text{drag coefficient}) \times (\text{intensity})^{-3} \tag{15}$$

In the derivation above a regular cubic packing of spheres has been considered, but the constant of proportionality is a function of the packing geometry in general.

In considering the applicability of Equation (14) or (15) to the present measurements, a number of questions arise immediately: Which Reynolds numbers can be considered sufficiently high for the reasoning to apply? To what extent can the contribution of skin friction to the drag coefficient C_D be ignored as small, and the pressure drag coefficient, known from a previous study (1), substituted? Will the drag coefficient tend to a constant value at high Reynolds numbers, as is the case for flow in rough

tubes, and will the turbulence intensity also tend to a constant value, making the Strouhal number a function of the geometry of the packing only? The present measurements are not sufficiently extensive to permit definite answers to these questions. However, the measured values of the Strouhal number, pressure drag coefficient, and intensity at the highest and lowest Reynolds numbers are not incompatible with the relation expressed in Equation (15).

At high wave numbers all spectra appear to have similar slopes. The band width limitation of the tape recorder for high Reynolds numbers, as well as the required wire length correction, make it difficult to be definite on the behavior of the spectrum, except that Kolmogoroff's $(-5/3)$ law at high wave numbers appears to be in general agreement with the measurements as determined.

Estimation of the Integral Scale of Turbulence

For isotropic turbulence, the longitudinal integral scale L_f is defined as

$$L_f = \int_0^\infty f(r)dr \tag{16}$$

where $f(r)$ is the dimensionless velocity correlation function

$$u'^2 f(r) = \overline{u(x)u(x+r)} \tag{17}$$

and r is the separation distance in the x direction

The one-dimensional energy spectral density function $F(k)$ is the Fourier transform of $f(r)$:

$$F(k) = u'^2 \int_{-\infty}^{+\infty} f(r)e^{2\pi ikr}dr \tag{18}$$

An alternative expression for the longitudinal integral scale is therefore

$$L_f = F(0)/2u'^2 \tag{19}$$

In isotropic turbulence, L_f is determined through extrapolation of the flat low wave number section of $F(k)$ to $k = 0$, or through the use of an expression for $F(k)$ due to von Karman (*20*) which is fitted to the higher wave number region of the spectrum. Alternately, it can be shown (reference *20*, Equation 3-138) that if L_e is the average size of the energy containing eddies, then according to von Karman's formula

$$L_f = 0.75\ L_e \tag{20}$$

This suggests taking the value k_e corresponding to the maximum in the spectrum, and writing

$$L_f = 0.75/k_e \tag{21}$$

These procedures are satisfactory if the spectra are similar and only a single parameter is required to characterize any particular spectrum. The measured spectra have a peaked appearance, and show other differences, such as narrower and broader peaks, as well. These differences can be taken into account if the method of Laurence (*21*) is used. [The uncertainty regarding the slope of the spectra at high wave numbers is such that one may consider the slope to be compatible with either the $(-5/3)$ law or Laurence's k^{-2} line, at different portions of the spectrum.] This leads to a value of the integral scale that is different from that defined in Equation (17), but Laurence found that it behaves in a manner similar to the usual integral scale of the turbulence. In fact, calculation of L_f according to Equation (22) gives values of L_f of the same order of magnitude as the values obtained through the method of Laurence. The appearance of the spectra is such that the particular value of k_e to be selected is not always obvious, and the fact that Laurence's method takes the general behavior of the spectrum into account over a larger range of wave numbers is another reason for the choice of the method to compare different spectra. The integral scale according to Laurence, which will be denoted by L_I, is shown below for two positions and two Reynolds numbers.

Reynolds number	Integral scale, cm.	Center coordinates X	Y	Z	Pore coordinates x	y	z
27,000	2.0	6.5	0.5	0.5	0	0	0
27,000	2.85	11.0	0.5	0.5	0	0	0
2,500	0.64	6.5	0.5	0.5	0	0	0
2,500	1.22	11.0	0.5	0.5	0	0	0

Since only one spectrum has been determined at a particular point, these determinations are of a qualitative value only but indicate that the resolution of the turbulent velocity field, especially at higher Reynolds numbers, should be adequate.

It is of some interest to compare the estimates of L_I with those of Mickley, Smith, and Korchak, obtained away from the void center at a point of maximum velocity. They found

N_{Re}	$\overline{U}$	I	L_f	$u'L_f$	Turbulent dispersion coefficient, D_e Radial $N_{Pe} = 11$	Axial $N_{Pe} = 2$
4,780	1024	0.26	0.27	70	261	1440
7,010	1423	0.24	0.28	98	383	2110

Since they used a rhombohedral packing, the corresponding flow passages were much narrower, and the ratio of integral scale to particle diameter ($d = 38$ mm.) was of the order of 0.07, compared to the ratio $L_I/d = 0.3$ for $N_{Re} = 27{,}000$ in the present study. Using the diameter of the largest inscribed circle between spheres as a characteristic pore length, one still finds that the ratio of integral scale to characteristic pore length is smaller for the rhombohedral packing, and this trend is only intensified if one chooses similarly the diameter of the smallest inscribed sphere for the cubic packing as a characteristic pore length. The relatively smaller integral scale for the rhombohedral packing indicates that the rhombohedral geometry apparently inhibits the existence of a particular range of large (as compared to pore dimensions) sizes of eddy associated with the energy-carrying range of eddy sizes, and the pronounced peak in the spectrum does not appear, which explains the appearance of the spectra reported by Mickley et al., as mentioned earlier.

Mickley et al. used values of 11 and 2 for the Peclet number to characterize the radial and axial dispersion coefficients, respectively. Defining the Peclet number as $v_0 d/D_e$, they found the values of D_e corresponding to the average pore velocity v_0 shown in the above table. The values of D_e calculated from $u'L_f$ are much smaller than those calculated from the Peclet number, and they conclude that the side-stepping of the fluid, as it passes between particles, is responsible for the higher values of D_e obtained from the dispersion experiments.

In the regular arrangement no obvious side-stepping should take place, the flow following in general a straight path encountering successively contractions and expansions. It is known (*6*) that in pipe flow the eddy diffusivity of the turbulence makes a negligible contribution to the axial dispersion. In a packed bed the eddy diffusivity is much higher on account of the higher turbulence intensity, but one would expect that the convective transport due to velocity gradients would still provide the major contribution to the axial dispersion.

From the values of the velocity, intensity, and integral scale at the center of the pore behind the sixth bank in

the present study, the values of the dispersion coefficient are found to be

N_{Re}	$u'L_I$	Turbulent dispersion coefficient, D_e Radial $N_{Pe} = 11$	Axial $N_{Pe} = 2$
27,000	760	800	4,400
2,500	28	75	410

The eddy diffusivity at the higher Reynolds number is of the same order of magnitude as the radial dispersion coefficient, but much smaller at the lower Reynolds number, suggesting a different type of flow behavior at $N_{Re} = 2{,}500$. This is further supported by the fact that the value of L_I/d was found to be 0.09 for the latter Reynolds number, compared with 0.3 for $N_{Re} = 27{,}000$.

Probability Density Function of the Velocity

The amplitude of the fluctuating velocity in a turbulent flow has an almost normal distribution. There is no reason to believe that the distribution would be different for turbulent flow in a packed bed, unless regular eddy shedding occurs, and some determinations of the flatness K of the probability density function have been made. On account of the asymmetry of some mean velocity profiles, the skewness of the probability density function, which indicates a relatively larger or smaller convection velocity than the mean velocity (for example, reference 22), had too erratic a behavior, and was not tabulated. The flatness K' of the time-differentiated fluctuating velocity $\dot{u}$ has also been computed. K and K' are defined as

$$K = \overline{u^4}/(\overline{u^2})^2, \quad K' = \overline{\dot{u}^4}/(\overline{\dot{u}^2})^2 \qquad (22)$$

The values of K and K' are tabulated in Tables 1 and 2.

For a normal distribution $K = 3$. In turbulent flows it is found that the flatness factors for the velocity derivatives $(\partial^s u/\partial x^s)$ increase with s. Batchelor (23) gives the average values as $K = 3$, 3.9, 4.9, 5.9, for $s = 0$, 1, 2, 3, respectively. $\dot{u}$ is taken to be an approximation for $U(\partial u/\partial x)$, with the limitations already discussed, following Equation (8).

Inspection of Tables 1 and 2 shows that at the center of the pores, the flatness factors K and K' are close to three for all pores and all Reynolds numbers, an exception being the pore behind the second bank of spheres. Considering the different types of spectrum obtained in the pore behind the first bank, it is conjectured that the observed peaks correspond to eddy shedding at a dominant frequency, but with random phase, phase differences being ignored in the power spectrum. The measurements behind the first bank are presumably made in the potential core of the jet formed behind the bank, and the measurements behind the second bank take place intermittently in the tailend of the potential core.

The values of K laterally across a pore behind the sixth bank is close to three for Reynolds numbers of 27,000, 10,000 and 5,000, and larger than three for the lowest Reynolds number of 2,500. The values of K' show a different behavior, and point to progressively larger values of K' with lower values of the Reynolds number in the regions of high shear and recirculating flow. The increase in K' at $N_{Re} = 27{,}000$ is comparable to the value of 3.9 quoted by Batchelor for the first derivative, but the increases at lower Reynolds numbers are much larger. The conclusion is that for turbulent Reynolds numbers ($N_{Re\lambda}$) below 100, the turbulent flow has an inhomogeneous structure compared to the flow at high turbulence Reynolds numbers.

CONCLUSIONS

The flow through the regular arrangement of ten banks of spheres has been described in detail with regard to mean velocity and turbulence intensity for the highest Reynolds number of 27,000. The measurements shown in Table 1*D* support and confirm the observations reported in a previous study (1) on pressure drag coefficients. In particular, the mean velocity profiles verify the existence of a large potential core in the pore following the first bank of spheres; the spreading of the jet in this pore is small. In the second pore the potential core is smaller, and the spreading of the jet increases. This behavior is accompanied by a marked increase in turbulence intensity; the latter very rapidly reaches a level high enough to cause a laminar-turbulent transition in the boundary layer, as reported by Torobin and Gauvin (2) and as inferred from the wide separation angle ψ (approximately 135 deg.) observed in the previous study (1).

The flow behavior at lower Reynolds numbers has been determined semiquantitatively only with respect to the flow at $N_{Re} = 27{,}000$. What remains to be done is a more intensive study of the flow in the fully developed flow region through a single pore of the bed at different Reynolds numbers, so as to obtain accurate comparisons for different Reynolds numbers of the mean velocity distribution, the turbulence intensity, and the various length scales of the turbulence. Such a study would remove the doubts regarding the trend of the intensity with Reynolds number. The present measurements at Reynolds numbers of 5,000 and 10,000, for example, agree qualitatively with Korchak's measurements at Reynolds numbers of 4,780 and 7,010 but show an opposite trend when the intensities at all four Reynolds numbers are considered. Also, the intensity profile flattens out at higher Reynolds numbers when the measurements at N_{Re} of 27,000 and 2,500 are compared, but the mean velocity profile appears to be more peaked. [Compare also the results on pressure drag coefficients between Reynolds numbers of 10,000 and 2,500 previously reported (1).]

The spectra of the fluctuating velocity in the regular and skewed arrangements, as well as the spectra behind the bed, are similar in showing a very pronounced peak, with no resemblance to the longitudinal spectra measured in isotropic turbulence. The similar appearance of spectra behind the regular arrangement compared to spectra in the bed is plausible as the change in flow pattern at the exit is one of degree rather than type. The flow deformation is different in the skewed arrangement, but the large voidage of the cubic arrangement apparently allows qualitatively similar flow behavior.

Apart from the peaked appearance of the spectra, no eddy shedding has been detected in or behind the bed, except for measurements behind the first bank at the lowest Reynolds numbers. Considering the appearance of the spectra and the flatness factors of the probability density function of the velocity, the flow appears to be fully turbulent at $N_{Re} = 27{,}000$, when the flatness factors K and K' are considered.

There are several pointers beside the high values of K and K' for $N_{Re} = 2{,}500$ to indicate a different structure for the turbulent flow. It is necessary to stress that the calculations for the turbulence Reynolds and Kolmogoroff scale were performed as if the turbulence behaved isotropically, which is very questionable for the low turbulence Reynolds number found at $N_{Re} = 2{,}500$. A different description of such turbulence is required to take the inhomogeneity into account. Such a procedure has been followed to describe the small-scale structure at very high turbulence Reynolds numbers by Obukhov (24) and Kolmogoroff (25). This inhomogeneity is a factor to consider in packed-bed applications involving reactions.

In the regular arrangement, the side-stepping of the

fluid particles is not nearly as obvious as in Mickley et al.'s rhombohedral packing. These authors ascribed the dispersion in a packed bed to the side-stepping of the fluid rather than to the turbulence. Calculating an eddy diffusivity in the same manner as these authors, that is, the product of the fluctuating velocity and the estimated longitudinal integral scale L_I, one arrives at radial eddy diffusivities that are of the same order of magnitude as those calculated from the Peclet number characterizing the dispersion through a packed bed. For the regular cubic arrangement, it appears that turbulence is certainly a contributing factor in the dispersion process, as the peaked velocity profiles will necessarily contribute to the axial dispersion.

ACKNOWLEDGMENT

Financial assistance from the National Research Council of Canada, the Commonwealth Scholarship and Fellowship Association, and the South African C.S.I.R. is gratefully acknowledged.

NOTATION

A, B, C, C' = constants
C_D = drag coefficient of sphere in bank
d = sphere diameter, cm.
D_e = turbulent dispersion coefficient, sq.cm./sec.
$E = E + e$ = instantaneous linearizer output, v.
$\overline{E}$ = mean linearizer output, v.
$\overline{E}_c$ = mean linearizer output during calibration, v.
e = fluctuating linearizer output, v.
$E( )$ = three-dimensional energy spectrum
$F( )$ = one-dimensional energy spectrum
$f( )$ = dimensionless longitudinal velocity correlation function
$I = u'/\overline{U}$ = local value of turbulence intensity
K = flatness factor of u
K' = flatness factor of du/dt
K^* = constant in Equation (1)
k = wave number, cm.$^{-1}$
$k_e = 1/L_e$ = wave number corresponding to L_e
L_e = length scale of energy-carrying eddies, cm.
L_f = longitudinal integral scale of turbulence, cm.
L_I = integral scale of turbulence according to Laurence (*21*), cm.
M = exponent in Equation (1)
n = frequency, hz.
N = exponent in Equation (3)
N_{Re} = Reynolds number of flow through bed, based on superficial velocity, $U_0 d/\nu$
n_e = frequency at which maximum in longitudinal spectrum occurs
N_{Pe} = Peclet number, $v_0 d/D_e$
Δp = pressure drop across bank, dynes/sq.cm.
P_0 = voidage or porosity
$\overline{Q}$ = magnitude of effective cooling velocity, cm./sec.
$\overline{Q}_c$ = magnitude of effective cooling velocity at calibration, cm./sec.
r = separation distance in direction (also coordinate in spherical coordinate system in Figure 2), cm.
R = operating resistance of hot wire, ohm
R_c = operating resistance of hot wire at calibration, ohm
s = index indicating order of derivation
t = time, sec.
u = fluctuating velocity in X direction, cm./sec.
$\dot{u} = du/dt$ = time derivative of u, cm./sec.^{2}
u' = root-mean-square value of u, cm./sec.
u'_c = representative value of average turbulence intensity in pore, cm./sec.
$\overline{U}$ = local mean velocity in X direction, cm./sec.
$\tilde{U}$ = normalized mean velocity, cm./sec.
U_0 = superficial velocity, cm./sec.
V = local mean velocity in Y direction, cm./sec.
$V^* = \overline{V}^* + v^*$ = instantaneous anemometer bridge voltage, v.
$\overline{V}^*$ = mean bridge voltage, v.
v^* = fluctuating bridge voltage, v.
$\overline{V}_c^*$ = bridge voltage during calibration, v.
$v_0 = U_0/P_0$ = average pore velocity, cm./sec.
$v_c = \beta U_0$ = characteristic pore velocity, cm./sec.
w = fluctuating velocity in Z direction, cm./sec.
x, y, z = rectangular coordinate system defining location in pore
X, Y, Z = rectangular coordinate system defining location in bed

Greek Letters

β = constant in Equation (12)
ϵ = rate of energy dissipation per unit volume
η = Kolmogoroff length scale, cm.
θ = coordinate in spherical coordinate system in Figure 2
μ = dynamic viscosity of fluid, g./(cm.)(sec.)
ν = kinematic viscosity of fluid, sq.cm./sec.
ρ = density of fluid, g./cu.cm.
σ = solidity of sphere bank
ϕ = coordinate in spherical coordinate system in Figure 2
$\psi = \pi - \phi$ = angle from front stagnation point

LITERATURE CITED

1. van der Merwe, D. F., and W. H. Gauvin, *AIChE J.*, **17**, No. 2, 402 (1971).
2. Torobin, L. B., and W. H. Gauvin *ibid.*, **7**, 615 (1961).
3. Clamen, A., and W. H. Gauvin, *ibid.*, **15**, 184 (1969).
4. Prausnitz, J. M., and R. H. Wilhelm, *Ind. Eng. Chem.*, **49**, 978 (1957).
5. Mickley, H. S., K. A. Smith and E. I. Korchak, *Chem. Eng. Sci.*, **20**, 237 (1965).
6. Taylor, G. I., "Scientific Papers," G. K. Batchelor, ed., Vol. II, Cambridge Univ. Press, England (1960).
7. Jolls, K. R., Ph.D. dissertation, Univ. Illinois, Urbana (1966).
8. van der Merwe, D. F., Ph.D. dissertation, McGill Univ., Montreal (1968).
9. Rose, W. G., *J. Appl. Mech.*, **29**, 554, 758 (1962).
10. Champagne, F. H., *Boeing Res. Lab. Document DI-82-0491* (1965).
11. Heskestad, G., *J. Appl. Mech.*, **32**, 735 (1965).
12. Corrsin, S., in "Handbuch der Physik," S. Fluegge, ed., Vol. VIII/2 Springer-Verlag, Berlin (1963).
13. Uberoi, M. S., and L. S. G. Kovasnay, *Quart. Appl. Math.*, **10**, 375 (1953).
14. Lin, C. C., *ibid.*, **10**, 295 (1953).
15. Corrsin, S., *NACA RM 58B11* (1958).
16. Lumley, J. L., *Phys. Fluids*, **8**, 1056 (1965).
17. Gagne, R. E., *NRC DME MK-18*, Natl. Res. Council, Ottawa, Canada (1966).
18. Cometta, G., *Tech. Rept. WT-21*, Brown Univ., Providence, R.I. (1957).
19. Owen, P. R., *J. Mech. Eng. Sci.*, **7**, 431 (1965).
20. Hinze, J. O., "Turbulence," Sect. 3-5, McGraw-Hill, New York (1959).
21. Laurence, J. C., *NACA Rept. 1292* (1956).
22. Davies, P.O.A.L., *A.I.A.A. J.*, **4**, 1971 (1966).
23. Batchelor, G. K., "The Theory of Homogeneous Turbulence," p. 184, Cambridge Univ. Press, England (1953).
24. Obukhov, A. M., *J. Fluid Mech.*, **13**, 77 (1962).
25. Kolmogoroff, A. N., *ibid.*, **13**, 82 (1962).

Manuscript received September 29, 1969; revision received February 16, 1970; paper accepted February 19, 1970.